Analysis of Artificial Viscosity Effects on Reacting Flows Using a Spectral Multidomain Technique

Michéle G. Macaraeg* and Craig L. Streett†
NASA Langley Research Center, Hampton, Virginia
and
M. Y. Hussaini‡
Institute for Computer Applications in Science and Engineering, Hampton, Virginia

Standard techniques used to model chemically reacting flows require an artificial viscosity for stability in the presence of strong shocks. The resulting shock is smeared over at least two computational cells, so that the thickness of the shock is dictated by the structure of the overall mesh and not the shock physics. Present-day upwind schemes, which may be nonoscillatory and monotonic, are inherently dissipative, so that artificial viscosity exists in their fundamental formulation. In this study, the effects of imposing an artificial thickness on a calculated shock is investigated. The present study incorporates a nonequilibrium chemistry model for air into a multidomain spectral Navier-Stokes calculation. The computation follows the chemical kinetics and flow kinematics of a gas passing through a fully resolved viscous shock wave at hypersonic Mach numbers. Because no artificial viscosity, either added or inherent, is needed for stability of the multidomain technique, the precise effect of this artifice on the chemical kinetics and relevant flow features is determined.

I. Introduction

SINCE the inception of the design of the Space Shuttle more than 15 years ago, there has been considerable progress in prediction methodologies. We are beginning to see increasing sophistication in chemically reacting flow methods that involve nonequilibrium and two-temperature chemical kinetics.[1,2] To couple a nonequilibrium chemistry model successfully with the flow kinematics, we must first fully understand the impact the numerical algorithm has on the problem at hand. Such an investigation has not been researched to date; this work addresses fundamental questions relevant to such understanding.

The standard techniques used to model chemically reacting or nonreacting flows are finite-difference or finite-volume methods. One feature shared by both techniques is the artificial viscosity needed in the presence of strong shocks. The effect the artificial viscosity has is to smear the shock over at least two computational cells. The size of these cells is not dictated by the shock physics but by the structure of the overall mesh. A true viscous shock has a finite physical thickness that is typically many orders of magnitude smaller than the grid used in large-scale computations.

The present-day upwind codes, which may be nonoscillatory and monotonic, are inherently dissipative, so that artificial viscosity exists in their fundamental formulation via averaging processes employed at the shock. The pencil-thin two-point shocks are important for capturing macroscopic features in a large-scale calculation but in no way resolve the shock structure or chemical kinetics in the relaxation zone. The fact that the shocks in these computations are sharp, rather than possessing a smooth distribution throughout, is indicative that resolution on all scales has not been achieved and that numerical artifices are in operation to capture the shock without oscillation. The impact of not resolving these features is investigated here. To study accurately the chemical kinetics occurring in the relaxation zone, the actual thickness of the shock must be modeled. Sufficient resolution must be incorporated in this zone, which is on the order of a few mean free paths for altitudes of roughly 45 k.

When air passes through a strong shock wave, there follows a conversion of energy of directed translational motion into other forms of energy, such as translation, rotation, vibration, and dissociation. Because the temperature of a gas depends on the energy of translation, when energy is transferred into this form, the temperature of the gas rises. If, at a later time, a portion of the energy of translation is converted into other modes, the temperature falls. Because of differences in the magnitude of the time required for the different processes to absorb their equilibrium amount of energy, considering them to occur separately and consecutively results in a good approximation.[5] The variation of temperature from its freestream value to its value following establishment of thermal equilibrium can, therefore, be represented as in the schematic given in Fig. 1.[3] Station 1 represents conditions in the freestream ahead of the shock wave, where the temperature is low enough to preclude appreciably excited vibration of the molecules. Rotation of the molecules is, however, completely excited. Station 2 represents conditions behind, but very close to, the shock wave. The thermal jump across the shock wave throws the translational and rotational degrees of freedom temporarily out of equilibrium, but only a few molecular collisions are required to establish equilibrium not only of the translational, but also of the rotational, degrees of freedom. Adjustment of the vibrational degrees of freedom occurs between stations 2 and 3. This process requires a number of collisions (or a time or distance) that are large compared to that required for adjustment of translation and rotation but small compared to that required for establishment of dissociation equilibrium. At station 3, vibration is fully established, but dissociation is only beginning. At station 4, sufficient time has elapsed for the dissociation of oxygen to reach equilibrium and, at station 5, the dissociation of nitrogen

Presented as Paper AIAA 87-1183 at the 8th Computational Fluid Dynamics Conference, Honolulu, HI, June 9-11, 1987; received June 26, 1987; revision received Dec. 22, 1987.

*Research Scientist, Computational Methods Branch. Member AIAA.
†Research Scientist, Theoretical Aerodynamics Branch. Member AIAA.
‡Chief Scientist. Fellow AIAA.

is in equilibrium, and the temperature has reached its equilibrium value. These relaxation pathways are transition zones that initiate the chemical kinetics that follow. The pertinent questions are: Does the artificial smearing of the shock envelop the transition region? If so, is the distribution of energies and chemical composition significantly altered to affect the chemical kinetics of the flow?

Figure 2 is a plot of data accumulated from shock-tube experiments.[4–6] Shock thickness and relaxation path lengths are plotted against Mach number in air. The data correspond to shock thicknesses and relaxation path lengths existing at an altitude of 35 km. As can be seen, the shock thickness at this altitude is within two or three orders of magnitude of these relaxation lengths. A typical calculation easily smears a shock over several orders of magnitude, which is sufficient to obliterate this important region. Though it is possible with standard finite-difference techniques to resolve the shock sufficiently so that vibrational relaxation can be modeled, a calculation for more than just a very small region will be computationally too expensive. To make such a calculation practical for full-scale application, the needed resolution must be attainable on a tractable grid. At the very least, present-day computations of chemically reacting flows should be paralleled by fundamental studies of the effects that factors inherent in the algorithm have on the relevant physics.

A methodology well suited for carrying out such a study is the spectral multidomain technique.[7] One of the strongest properties of spectral methods is their exponential rate of convergence and high-order accuracy on relatively coarse meshes.[8] Extensions of their application to include capturing regions of high gradient and modeling complex geometries have recently been attainable owing to the spectral multidomain technique developed by Macaraeg and Streett.[9] The multidomain technique interfaces regions with independent discretizations, while maintaining spectral accuracy and an exponential rate of error decay. Adjoining regions are interfaced by enforcing a global flux balance, which preserves high-order continuity of the solution. This interface technique maintains spectral accuracy, even when mappings and/or domain sizes are radically different across the interface. Such advantages are needed when computing chemically reacting flows, which can display widely disparate temporal and spatial scales owing to fast chemical reaction as opposed to the macroscopic scales associated with the hydrodynamics.

II. Multidomain Spectral Technique

Numerical flow simulations using spectral methods is well documented in the literature.[10] In a spectral technique, points in the flowfield are represented as a linear combination of an approximate set of basis functions defined over the entire domain. The advantage of this global accuracy is the need for many fewer grid points while much finer resolution is attained. There are basically three techniques available to project a continuum equation into a spectral representation.[11] These are spectral Galerkin, tau, and collocation. At present, spectral collocation is at least a factor of two faster than Galerkin or tau and is most appropriate for numerical flow simulations.[12] Spectral collocation involves solving the equations in physical space rather than in the spectral space with transforms used only to evaluate derivatives.[13,14] This allows relative ease of evaluating nonlinear terms or terms involving nonconstant coefficients. In addition, boundary conditions are exactly the physical boundary conditions associated with the analytical partial differential equation.

One drawback to classical single-domain spectral techniques has been the requirement that a complicated physical domain must map onto a simple computational domain for discretization. This mapping must be smooth if the high-order accuracy and exponential convergence rates associated with spectral methods are to be preserved.[15] Additionally, even smooth stretching transformations can decrease the accuracy of a spectral method if the stretching is severe.[16] Such stretchings would be required to resolve the thin viscous region in an external aerodynamic problem or the widely disparate scales that occur in chemically reacting flows. These restrictions are overcome in the present method by splitting the domain into regions, each of which preserves the advantages of spectral collocation, and allow the ratio of mesh spacings between regions to be several orders of magnitude higher than are allowable in a single domain.

A number of other spectral domain decomposition techniques have appeared in the literature. For example, the spectral element method that applies finite-element methodology using Galerkin spectral discretization in the variational formulation within elements is a popular technique.[17,18] One drawback with this technique is that it uses a split Galerkin-collocation discretization, which restricts its application to convection-diffusion problems for incompressible flows. The spectral element method in practice is used in a manner similar to classical finite-element techniques: low-order internal discretization using many elements with no internal stretchings to improve resolution. In addition, each element contains the same number of collocation points. Other domain decomposition techniques involve explicit enforcement of C^1 continuity

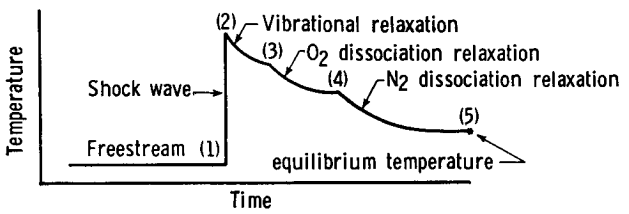

Fig. 1 Schematic of relaxation zones for nonequilibrium air.

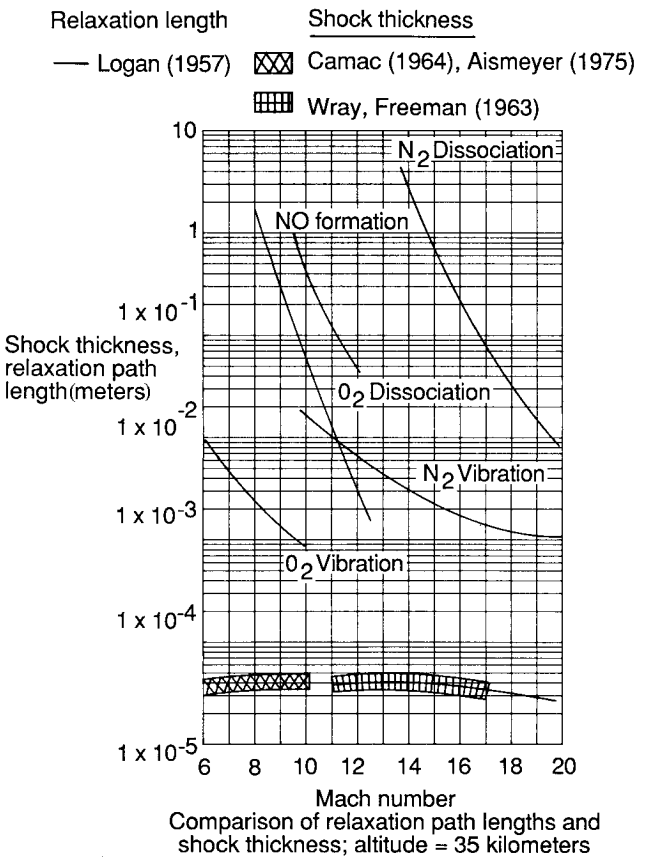

Comparison of relaxation path lengths and shock thickness; altitude = 35 kilometers

Fig. 2 Comparison of relaxation path lengths and shock thicknesses; altitude = 35 km.

across the interface.[19,20] It is not clear how well these techniques perform for strongly convection-dominated problems; the second author's experience with such techniques[21] has shown them to be not entirely satisfactory.

The multidomain spectral technique overcomes the above-mentioned restrictions by splitting the domain into regions with independent collocation discretizations, each of which preserves the advantages of spectral collocation, and allow the ratio of the mesh spacings between regions to be several orders of magnitude higher than allowable in a single domain. The partitioning results in three classes of points: the interior points, where collocation of the equation is applied; boundary points, where the physical boundary conditions are applied; and interface points, which satisfy a global flux balance across adjoining subdomains and preserve high-order continuity of the solution. The global flux balance utilizes an integral, performed spectrally, of the discrete equation across the interface.[22] In the multidimensional case, this integration is performed along the coordinate line perpendicular to the interface. If adjoining domains have coordinate lines perpendicular to the interface that do not line up, the coordinate points from the domain with the fewer number of points are spectrally interpolated from the fine grid onto the coarse grid. To close the equation set, continuity of the solution and the flux is assumed at the interface. The total system of interface relations has a block structure, each block spanning a single interface between a pair of adjoining domains. Because the discretizations interior to each domain are solved uncoupled from each other and because the interface relation has a block structure, the solution scheme can be adapted to the particular requirement for each domain. Iterative and noniterative schemes have been developed to solve the combined interior/interface system. Details of the algorithm, as well as comparisons between the present method, spectral element, and single domain collocation, are given in Ref. 7.

III. Numerical Model

The preceding technique is used to model the chemical kinetics and flow kinematics of a nonionized air mixture (O2, N2, NO, O, and N) passing through a fully resolved shock wave, thus alleviating the need for artificial viscosity. The governing equations are the quasi-one-dimensional Navier-Stokes equations[23] and species conservation equation.[1] The quasi-one-dimensional form is used to provide an artifice for controlling the shock location in the physical space for this otherwise indeterminate problem. The equations are nondimensionalized by the following scalings: state and transport parameters are divided by their dimensional freestream values.

The viscosity of each of the individual species is calculated from a curve-fit relation.[24] Similarly, curve fits are used to obtain specific heats, internal energies, and enthalpies.[25,26] The thermal conductivity of each specie is calculated from the Euken semiempirical formula using the specie's viscosity and specific heat. Appropriate mixture rules are next used to obtain the previously-mentioned transport properties of the mixture.[27] Experimental values of bulk viscosities, as obtained from acoustical interferometry and related experiments, are taken from Truesdell.[28]

In the present work, the diffusion model is limited to binary diffusion, with the binary diffusion coefficients specified by the Lewis number. The value of the Lewis number used is 1.4, an accurate approximation for binary diffusion under the conditions studied.[29]

The temperature range under study will not exceed 4000 K for conditions at an altitude of approximately 55 km. Therefore, ionization reactions, which occur at roughly 9000 K, are not included. The chemical reactions utilized for the non-ionized air mixture are impact dissociation and exchange reactions. The seventeen reactions included in the present study can be found in Ref. 1, which also lists ionization reactions. The constants needed to evaluate reaction rates are given in Ref. 2.

Initial conditions are obtained from a spectral multidomain equilibrium code written for the above-mentioned problem. These governing equations may be found in Ref. 23. Transport properties are obtained in the manner previously discussed. The routines of Ref. 25 generalized for air are used to obtain equilibrium concentrations.

IV. Numerical Algorithm

The multidomain discretization involves three independent subdomains, with the shock located in the center subdomain. Shock jump conditions are obtained by an iterative procedure to solve the Rankine-Hugoniot relations for real air.

A direct inversion of the coupled system is used to obtain a fully implicit method. The conserved variables are written in delta form, and a pseudo time iteration using a backward Euler scheme is used to obtain the steady-state solution.[22]

V. Method Verification

Validity of the multidomain Navier-Stokes algorithm is demonstrated by comparison with experiment. A low-density wind-tunnel study of shock-wave structure and relaxation phenomena in gases was conducted by Sherman.[30] The experiment measured shock wave profiles recorded in terms of the variation in the equilibrium temperature of a small diameter wire oriented parallel to the plane of the shock, as the wire is moved through the shock zone. Freestream Mach number is 1.98. For this test case, a Navier-Stokes spectral multidomain calculation is performed for a perfect gas with temperature-dependent properties and a nonzero bulk viscosity corresponding to air.[28] A comparison with experimental temperatures normalized by the freestream temperature vs normalized distance is given in Fig. 3. The experimental data points are represented by the

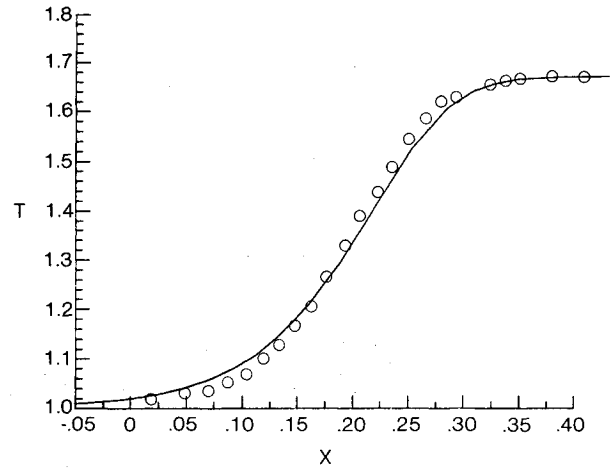

Fig. 3 Comparison of multidomain Navier-Stokes calculation with experimentally obtained temperatures; $M_\infty = 1.98$, $Re = 260$/m. Discretization 11/21/11, interfaces at −0.15 and 0.3.

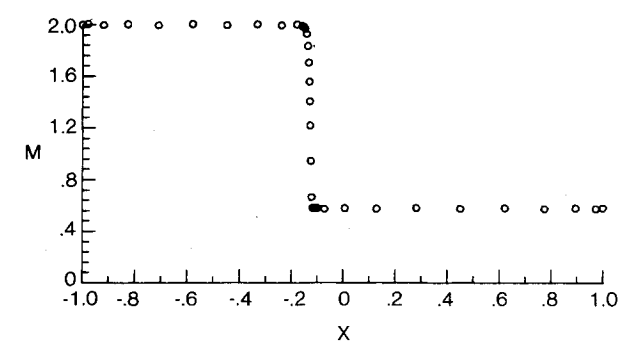

Fig. 4 Computed solution for $Re = 3250$/m; discretization 11/17/11, interface at −0.15 and −0.1.

open symbols. The numerical results fall within a symbol width of the data. The multidomain technique used three domains. The center domain, located between $x = -0.15$ and $x = 0.3$, contains 21 points; the outer domains contain 11 points each. The computational domain spans -1 to 1. The unit Reynolds number (m^{-1}) of the flow is 260 (80 ft^{-1}). The plot is of Mach number vs Grad's dimensionless distance X, which may be written as[30]

$$X = (4\varepsilon/35)R^*x$$

where ε is the shock strength,

$$\varepsilon = [15(M_1^2 - 1)/(3 + 5M_1^2)]$$

and the viscosity in the unit Reynolds number R^* is evaluated at

$$T^* = [2/(\gamma + 1)]T^0$$

where T^0 is the stagnation temperature, and γ is the ratio of specific heats.

A calculation for a unit Reynolds number of 3250 m^{-1} (1000 ft^{-1}) is given in Fig. 4, showing the ability of the method to accurately resolve strong gradients without numerical oscillations. Three domains are again used; the center domain contains 17 points, the outer domains contain 11 points each. The interfaces are located at -0.15 and -0.1.

VI. Results

The case to be discussed with respect to effects of nonequilibrium assumptions on the flow/chemistry is for $M_\infty = 11.0$, $T_\infty = 350$ K, and $\rho_\infty = 6 \times 10^{-8}$ g/cm^3. These conditions invoke primarily O_2 dissociations, with N_2 dissociations just beginning. Temperatures are not yet high enough for ionization to occur, so that electronic energy modes remain unexcited.

Typical discretizations in this study are 15, 27, and 33 points. The freestream postshock domain utilizes 15 points. A physical shock thickness is modeled in the center domain with 27 points in a zone of roughly 10^{-5} m, and the relaxation zone incorporates 33 points in a distance of 10^{-4} to 10^{-3} m. Exhaustive grid resolution studies reveal this to be the minimum discretization required to resolve the scales of the shock and the chemical kinetics of the relaxation zone. The backward-Euler implicit time-stepping algorithm typically required less than 2000 iterations to converge from an equilibrium starting solution, with at least an eight order of magnitude reduction in maximum residual.

The study of the effect of artificial viscosity on the flow physics is carried out by adding the equivalent of second-order artificial viscosity to the momentum, energy, and species' concentration equations, by increasing the value of the physical viscosity. The amount of artificial viscosity introduced is such that the shock is spread out to a thickness about three orders of magnitude wider than the fully resolved no-artificial-viscosity solution. This width is chosen to represent the grid spacing of a typical shockcapturing computation on a full-scale configuration, such as the one mentioned in the Introduction. Figures 5a and 5b show the Mach number and temperature profiles for the resolved-shock and smeared-shock cases, respectively; note that the entire physical domain is shown in Fig. 5b, whereas only the near-shock region on a greatly expanded scale is plotted in Fig. 5a. For the resolved-shock case, endpoints are at -1 and 200, and interface points are at -0.3 and 0.1. The interface locations for the smeared shock case are at 65 and 100, with endpoints at 0 and 270. The most important feature to note in comparing these profiles is the 20% reduction in the temperature overshoot as a result of the artificial viscos-

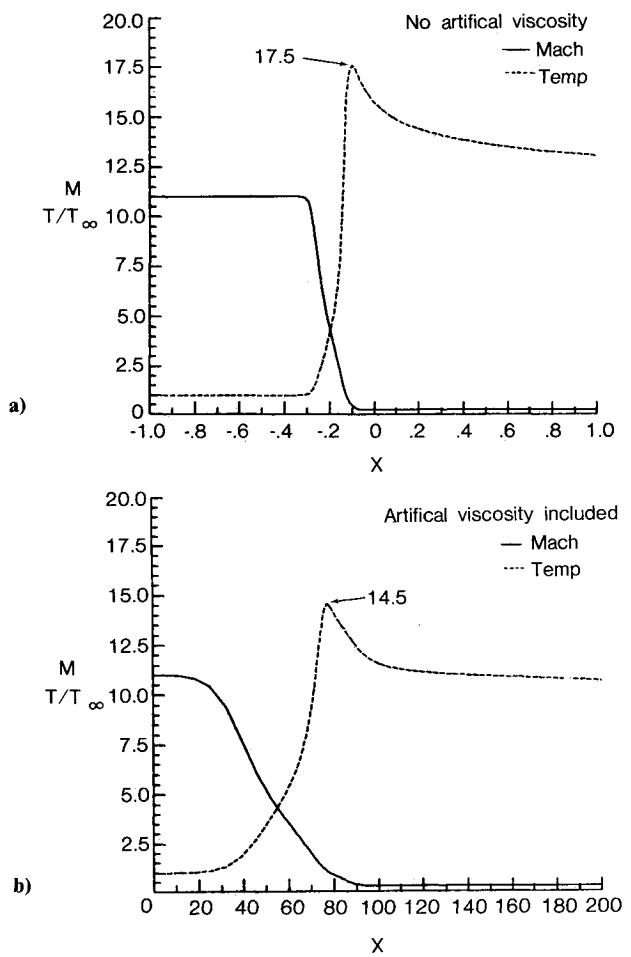

Fig. 5 Comparison of temperature and Mach number profiles for calculations: a) without artificial viscosity, and b) with artificial viscosity.

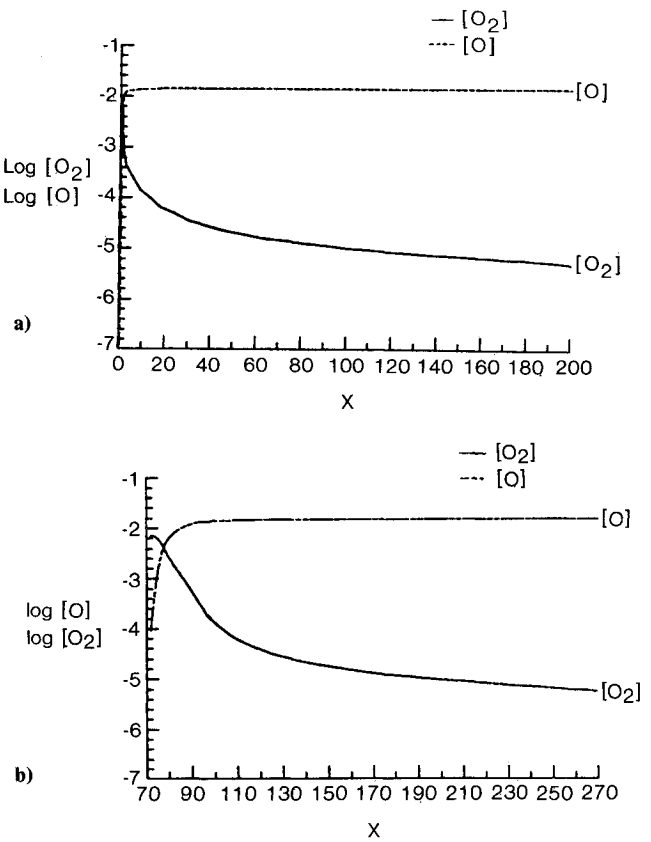

Fig. 6 Comparison of relaxation pathway for $[O_2]$ and [O] for calculations: a) without artificial viscosity, and b) with artificial viscosity.

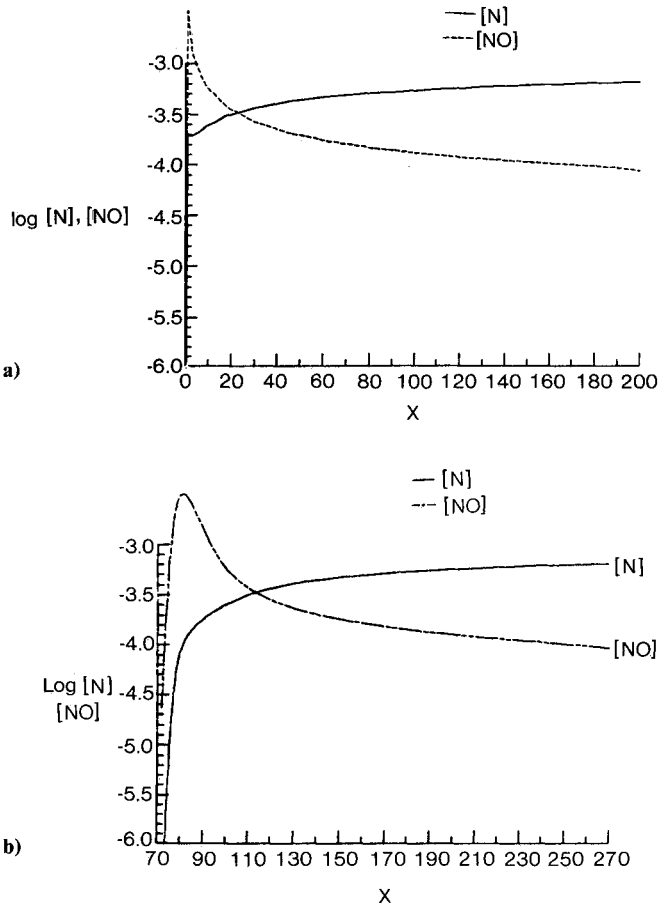

Fig. 7 Comparison of relaxation pathway for [N] and [NO] from calculations: a) without artificial viscosity, and b) with artificial viscosity.

ity. We conjecture that this is not the result of simple smearing but is produced by the change in the relative magnitude of the spatial scales of the flow kinematics and chemical kinetics. The temperature overshoot is produced by the conversion of kinetic to thermal energy on a scale too small for the chemistry to respond. Thus, the near-shock chemistry is essentially frozen, and the ratio of enthalpy to internal energy remains near its freestream value. The chemical reactions then begin to respond on their own scale, as dictated by the reaction rate constants used in the model. A fraction of this thermal energy is absorbed by the molecules undergoing reaction, lowering the temperature. When the shock is smeared, the conversion of kinetic into thermal energy occurs on a scale nearer that on which the reactions operate and, therefore, some of this energy is absorbed by the reactions while the release of energy is still taking place. This reduces the overshoot in temperature.

Simple smearing of the shock from the artificial viscosity cannot account for this effect, as can be realized by considering an equilibrium calculation. For such a calculation, only one spatial scale exists and is dictated by the Reynolds number. Thus, a change in scale or a change in *Re* is equivalent. Introduction of second-order artificial viscosity may, of course, be looked at as lowering the effective *Re* of a calculation. Thus, any change in the shock profile by the introduction of artificial viscosity that cannot be accounted for by a simple scale change must be attributed to an alteration of the interplay between flow kinematics and chemical kinetic scales. This effect can be expected to strengthen with increasing Mach number.

For the Mach 11 case considered here, although the path along which the chemistry relaxes is significantly altered in the near-shock region, the chemical end states from the computations with and without artificial viscosity are within 3–4% of each other. This can be seen in Figs. 6a, 6b, 7a, and 7b, which show the profiles of $[O_2]$ and [O] (Figs. 6a and 6b) and [N] and [NO] (Figs. 7a and 7b) in the relaxation zone. This is not to say, however, that this situation will always occur, especially for higher Mach numbers, where electronic excitation (ionization) occurs. The reduction in the temperature overshoot could result in a large enough change in the relaxation path to affect the end state. For example, ionization reactions will not occur if artificial viscosity decreases this overshoot so that temperatures are not sufficiently high to initiate its onset.

VII. Discussion

Although smooth, accurate, and consistent solutions have been obtained for the concentrations of species in the post-shock region, which is the region of interest here, we feel the solutions are not entirely satisfactory in the upstream region and in the shock. The difficulty is that the range over which the concentrations of several of the species vary is too large to be accurately represented, given the Cray single-precision (64-bit) computations employed. Although iterative improvement is used in the Jacobian inversion of the time-stepping scheme to reduce the effects of finite word length, the usable dynamic range of the solution was limited to about six orders of magnitude. In the solution for [O], for example, the end state concentration is about 10^{-2}; the [O] solution in the freestream, however, oscillates at about $\pm 10^{-8}$, where the equilibrium concentration should be about 10^{-34}. This extremely small oscillation disappears in the shock region when reactions begin to take place, but it is still something of an annoyance. Figure 3 of Ref. 1 also shows evidence of this difficulty in the near-shock region. We are investigating recasting species' concentration equations in terms of the logarithm of the concentrations to better resolve the entire dynamic range of the solution.

References

[1]Park, C., "On Convergence of Computation of Chemically Reacting Flows," AIAA Paper 85-0247, 1985.

[2]Gnoffo, P. A. and McCandless, R. S., "Three-Dimensional AOTV Flowfields in Chemical Nonequilibrium," AIAA Paper 86-0230, 1985.

[3]Wood, G. P., "Calculation of the Rate of Thermal Dissociation of Air Behind Normal Shock Waves at Mach Numbers of 10, 12 and 14," NACA TN-3634, 1956.

[4]Logan, J. G., "Relaxation Phenomena in Hypersonic Aerodynamics," IAS Preprint 728, 1957.

[5]Alsmeyer, H., "Density Profiles in Argon and Nitrogen Shock Waves," *Journal of Fluid Mechanics*, Vol. 74, March 1976.

[6]Camac, N., "Argon and Nitrogen Shock Thicknesses," Preprint 64-35, Aerospace Sciences Meeting, 1964.

[7]Macaraeg, M. G. and Streett, C. L., "Improvements in Spectral Collocation Discretization Through a Multiple Domain Technique," *Applied Numerical Mathematics*, Vol. 2, No. 2, April 1986.

[8]Hussaini, M. Y., Streett, C. L., and Zang, T. A., "Spectral Methods for Partial Differential Equations," NASA CR-172248, 1983.

[9]Macaraeg, M. G. and Streett, C. L., "A Spectral Multi-Domain Technique with Application to Generalized Curvilinear Coordinates," *Sixth International Symposium on Finite Element Methods in Flow Problems*, Paper No. 14 1986.

[10]Streett, C. L., "Spectral Methods and Their Implementation to Solution of Aerodynamic and Fluid Mechanic Problems," *International Journal for Numerical Methods in Fluids*, Vol. 7, Oct. 1987, pp. 1159-1189.

[11]Gottlieb, D. and Orszag, S. A., *Numerical Analysis of Spectral Methods: Theory and Applications*, Society for Industrial and Applied Mathematics, Philadelphia, PA, 1977.

[12]Orszag, S., "Numerical Simulation of Incompressible Flows Within Simple Boundaries: 1. Galerkin (Spectral) Representation," *Studies in Applied Mathematics*, Vol. 50, Dec. 1971, pp. 293-327.

[13]Orszag, S. and Israeli, M., "Numerical Flow Simulation by Spectral Methods," *Proceedings of the Symposium on Numerical Models of Ocean Circulations*, National Academy of Sciences, Washington, DC, 1972, pp. 284-300.

[14]Orszag, S., "Fourier Series on Spheres," *Monthly Weather Review*, Vol. 102, Oct. 1974, pp. 56-75.

[15]Streett, C. L., "A Spectral Method for the Solution of Transonic Potential Flow About an Arbitrary Two-Dimensional Airfoil," AIAA Paper 83-1949-CP, 1983.

[16]Streett, C. L., Zang, T. A., and Hussaini, M. Y., "Spectral Methods for Solution of the Boundary-Layer Equations," AIAA Paper 84-0171, 1984.

[17]Patera, A., "A Spectral Element Method for Fluid Dynamics: Laminar Flow in a Channel Expansion," *Journal of Computational Physics*, Vol. 54, Sept. 1984.

[18]Ghaddar, N., Patera, A. T., and Mikic, B., "Heat Transfer Enhancement in Oscillating Flow in a Grooved Channel," AIAA Paper 84-0495, 1984.

[19]Metivet, B. and Morchoisne, Y., "Multi-Domain Spectral Techniques for Viscous Flow Calculations," *Proceedings of the 4th Conference on Numerical Methods in Fluid Dynamics*, Pineridge Press, Swansea, UK, 1981.

[20]Migliore, H. H. and McReynolds, E. G., "Multi-Element Collocation Solution for Convective Dominated Transport," *Numerical Methods in Laminar and Turbulent Flows*, edited by C. Taylor, Wiley, Boston, MA, 1983.

[21]Gottlieb, D. L., Lustman, L., and Streett, C. L., "Spectral Methods for Two-Dimensional Shocks," Institute for Computer Applications in Science and Engineering Rept. 82-83, 1982.

[22]Macaraeg, M. G. and Streett, C. L., "A Spectral Multi-Domain Technique for Viscous Compressible Reacting Flows," *International Journal for Numerical Methods in Fluids*, June, 1987.

[23]Davy, W. C., Lombard, C. K., and Green, M. J., "Forebody and Base Real-Gas Flow in Severe Planetary Entry by a Factored Implicit Numerical Method," AIAA Paper 81-0282, 1981.

[24]Blottner, F. G., "Nonequilibrium Laminar Boundary Layer Flow of Ionized Air," General Electric Rept. R645D56, 1964.

[25]Erickson, W. D. and Prabhu, R. K., "Rapid Combustion of Chemical Equilibrium Composition: An Application to Hydrocarbon Combustion," *AIChE, Journal*, Vol. 32, Oct. 1986.

[26]*Jannaf Tables,* Thermochemical Data, Dow Chemical Co., Sept. 1977.

[27]Bird, R. B., Stewart, W. E., and Lightfoot, E. N., *Transport Phenomena*, Wiley, New York, 1966.

[28]Truesdell, C., "Precise Theory of the Absorption and Dispersion of Forces Plan Infinitesimal Waves According to the Navier-Stokes Equations," *Journal of Rational Mechanics and Analysis*, Vol. 2, Jan. 1953.

[29]Kays, W. M. and Crawford, M. E., "Convective Heat and Mass Transfer," 2nd ed., McGraw-Hill, New York, 1980.

[30]Sherman, F. S., "A Low Density Wind-Tunnel Study of Shock Wave Structure and Relaxation Phenomena in Gases," NACA TN-3298, 1955.